Received: 16 May 2018 | Revised: 6 September 2018 | Accepted: 27 September 2018

DOI: 10.1002/rra.3370

RESEARCH ARTICLE

WILEY

Bridging the lab-field interface in fluvial morphology at patch-scale: Using close-range photogrammetry to assess surface replication and vegetation influence

Jane Groom | Heide Friedrich

Department of Civil and Environmental Engineering, University of Auckland, Auckland, New Zealand

Correspondence
Jane Groom, Department of Civil and Environmental Engineering, University of Auckland, Auckland, New Zealand.
Email: jgro800@aucklanduni.ac.nz

Funding information
Royal Society of New Zealand, Grant/Award Number: UOA1412; Marsden Fund

Abstract

In fluvial research, comparisons of laboratory and field data sets are rare or outdated; therefore, future research would benefit from the integration of laboratory and field data sets. We use close-range photogrammetry as a tool to help bridge that interface. Close-range photogrammetry is a technique that is readily applied in both laboratory and field environments to capture submillimetre topographic data of natural and replica surfaces of gravel-bed rivers. Digital Elevation Models (DEMs) of difference (DoDs) are presented to quantitatively assess the replicability of four surfaces, using the casting process. Replication results with accuracies of <35 mm, including observed localized areas of particle dislodgement, suggest casting is a suitable process to integrate laboratory and field data sets in fluvial morphology, allowing natural surfaces (e.g., from the field) to be analysed in a controlled laboratory environment. This enables the isolation of parameters, such as the microtopography of the surface or water submergence. Further, we highlight the importance of considerations of the wider scale morphology required to contextualize patch-scale field research using close-range photogrammetry. We demonstrate this with an example of the influence of vegetation on DEM quality and roughness statistics. These wider morphological features are difficult to simulate in the laboratory, albeit have a control on patch-scale processes. The successful replication of natural surfaces using casting and the use of tools such as close-range photogrammetry provide a bridge for future research that requires the integration of laboratory experiments, field experiments, and numerical modelling.

KEYWORDS

casting, digital elevation model (DEM), close-range photogrammetry, field, laboratory

1 | INTRODUCTION

Fluvial research is undertaken in both laboratory and field environments, with an observed increase in the number of field studies (Piégay, Kondolf, Minear, & Vaudor, 2015). Laboratory experiments (i.e., experimental work) have enhanced knowledge of several aspects in fluvial science, including grain motion, flow turbulence, bed arrangement, armour layers, and near-bed structures, and are seen as a bridge between complex field experiments and simplified numerical models (Yager, Kenworthy, & Monsalve, 2015). Experimental work is advantageous due to the ability to identify controls on certain parameters (Thompson, Norton, & Hawkins, 1998; Yager et al., 2015). However, laboratory experiments are not quintessential of the natural environment, influencing the transferability of results between environments (Basile, Ciollaro, & Coppola, 2003; Klotz, Seiler, Moser, & Neumaier, 1980; Thompson et al.,

1998), particularly for ecological studies of animal behaviour (Rice, Lancaster, & Kemp, 2010).

Bridging the interface between laboratory and field experiments is facilitated using a casting technique to replicate the natural surface topography (Buffin-Bélanger, Reid, Rice, Chandler, & Lancaster, 2003; Chandler, Buffin-Bélanger, Rice, Reid, & Graham, 2003). Development of the casting technique and materials used produced replica surfaces that were visually deemed representative of the surface topography (Spiller, Rüther, & Baumann, 2012). Subsequently, casts are analysed in the laboratory to enhance the understanding of how topography influences flow properties (Rice, Buffin-Bélanger, & Reid, 2014), with recent quantification of flows over both permeable and impermeable beds (i.e., casts) providing novel insights into fundamental hydrodynamic differences in the near-bed region of gravel-bed rivers (Cooper, Ockleford, Rice, & Powell, 2017).

Quantification of the surface topography uses technologies such as laser scanning, structure from motion (SfM), and close-range photogrammetry to obtain a 3D model of the surface (Bertin & Friedrich, 2014; Hodge, Brasington, & Richards, 2009a). Close-range photogrammetry is implemented successfully in both laboratory (Bertin & Friedrich, 2014; Brasington & Smart, 2003; Butler, Lane, & Chandler, 2001; Chandler, Shiono, Rameshwaren, & Lane, 2001) and field environments (Bertin & Friedrich, 2016; Butler, Lane, & Chandler, 1998; Carbonneau, Lane, & Bergeron, 2003; Groom, Bertin, & Friedrich, 2018), with submillimetre accuracies. The roughness of a surface can be quantified, with multiple scales of roughness existing in a river, including reach scale (e.g., woody debris and areas of sediment deposition), bedform scale (e.g., clusters of particles), and grain scale (Aberle, Nikora, Henning, Ettmer, & Hentschel, 2010). The distinction between the latter are reflected in Figure 1, with a focus herein on grain-scale roughness.

Patch-scale roughness research (typically covering 0.1–1 m^2) requires context of the wider scale morphological features (Church, Hassan, & Wolcott, 1998), including vegetation or the presence of man-made features, for example, as the feedbacks within river channels result in morphology, sedimentation, and flow properties influencing the patch-scale surface roughness (Ashworth & Ferguson, 1986; Hardy, 2006). Vegetation is addressed differently throughout the existing body of literature. Studies actively avoid areas of vegetation (Huang & Wang, 2012), completely remove vegetation from their area of interest (Wickham & Petrie, 2015; Yochum, Bledsoe, Wohl, & David, 2014) or interpolate pixels deemed to be vegetation (Lane, James, & Crowell, 2000). Larger scale studies, such as those using laser scanning, use filtering algorithms to remove vegetation from data (Brasington, Vericat, & Rychkov, 2012). Therefore, field research is plagued with issues of vegetation, albeit there is limited information in regard to the effect of vegetation on roughness analysis, and the presence of vegetation is often neglected from laboratory-based research.

This paper will address two aims:

1. Evaluate the developed casting technique, and quantify its suitability to replicate surface roughness of laboratory and field surfaces.
2. Consider the morphological factors, namely, vegetation, affecting patch-scale dynamics in a field environment.

2 | METHODOLOGY

2.1 | Natural surfaces

Laboratory surfaces were created in a 19-m long, 0.45-m wide flume in the Water Engineering Laboratory at the University of Auckland. Two surfaces were armoured naturally for 67.5 hr under constant flow rate (Q = 95 L/s) and water depth (0.245 m). Sediment size ranged from D_{16A} 5 mm to D_{90A} 25 mm, with a median grain size (D_{50A}) of 16 mm, and D_{16A} < 2 mm to D_{90A} 41 mm, with a median grain size (D_{50A}) of 17 mm, for Lab 1 and Lab 2, respectively. The subscript "$_A$" indicates surface sediment from the armour layer, rather than the bulk sediment. Sediment size was determined from a single vertical photograph in the image analysis tool Basegrain®, which uses automatic grain separation and a line-sampling method to obtain the sediment distribution of over 400 detected grains (Detert & Weitbrecht, 2012).

Field surfaces, Field 1 and Field 2, were obtained from an exposed gravel bar in the Whakatiwai Stream, which is a small gravel-bed river in northeast North Island, New Zealand. Data have previously been collected with close-range photogrammetry at this site, where full details of the field site can be found (Bertin & Friedrich, 2016; Groom et al., 2018). The sediment is predominantly gravel, with a range of sediment size (from ~10 to ~200 mm), and includes patches of sand and large boulders. The analysed patches sediment size ranged from D_{16A} < 2 mm and D_{90A} 58 mm (D_{50A} = 18 mm) for Field 1 and D_{16A} < 2 mm to D_{90A} 32 mm (D_{50A} = 16 mm) for Field 2. To ensure the gravel bar of interest had been water worked, data were collected after a significant rain event, with evidence of trash lines along the banks, suggesting the water levels had been significantly higher than the water levels on the day. Data collection was undertaken during the winter months to ensure minimal vegetation presence.

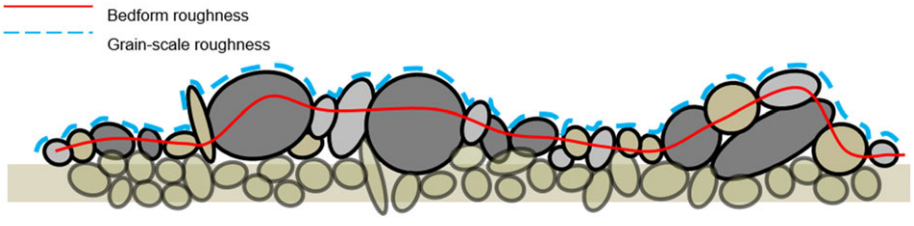

FIGURE 1 Schematic of grain-scale roughness and bedform roughness [Colour figure can be viewed at wileyonlinelibrary.com]

2.2 | Topographic data collection

Close-range photogrammetry uses two consumer grade (i.e., inexpensive) Nikon D5100 cameras with 20-mm Nikkor lenses installed in stereo above the surface (Bertin, 2016; Bertin & Friedrich, 2014; Bertin, Friedrich, Delmas, & Chan, 2013; Bertin, Friedrich, Delmas, Chan, & Gimel'farb, 2015) to capture an area of 350 mm (transverse) by 500 mm (downstream). Cameras were installed on a moving frame (laboratory) and tripods (field) (Bertin & Friedrich, 2016; Groom et al., 2018) to facilitate the collection of three sets of stereo images (30% overlap) merged together for a larger areal coverage (Bertin, Friedrich, & Delmas, 2016).

Cameras were calibrated (Zhang, 2000) with a mean rectification error of <0.5 pixel. Images were rectified and stereo matched (using the symmetric dynamic programming stereo (SDPS) algorithm) to produced point clouds (Gimel'farb, 2002) that were interpolated onto grids of 0.2 mm and subsequently 1 mm to generate digital elevation models (DEMs). Quality assurance on each DEM included the removal of outliers using a mean elevation difference parameter and bi-cubic spline interpolation (Hodge, Brasington, & Richards, 2009b). Finally, DEMs were detrended bi-linearly to remove planar trends larger than the grain-scale topography, such as experimental setup misalignment or bed slope (Bertin et al., 2015)

2.3 | Replica surfaces

The casting materials used and process undertaken followed that outlined in previous work (Spiller et al., 2012). A liquid two-component silicone rubber was used to create negative moulds of the surfaces (Figure 2). Mixing was completed for 8 min to increase the viscosity of the liquid before it is poured slowly onto the bed. The surface was outlined by an acrylic frame, with any gaps between the frame and the surface (resulting from the topographic irregularities), reduced by using plastic sheets taped to the side of the frame, and weighed down by sand. This was to minimize the seepage of moulding material and keep the silicone confined to the area within the frame. The same frame was used in both the lab and the field, ensuring the replica surfaces were the same dimensions (900-mm length and 350-mm width); in the flume, this ensured the effect of flume walls was removed.

Once the silicone covered the complete surface, it was left to set for 1 hr before being peeled off the surface, which destroys the structure of the natural bed underneath. The negative mould is cleaned of all stones, to ensure the imprint of the surface topography is reached, and placed into a frame with a base before the casting material is poured into the mould. The casting material was polyurethane resin, with a fine powdered filler added, which has been suggested to avoid shrinkage. No dye was added to the resin to make the first, white, cast (Figure 3a). However, subsequently, we experienced that when using close-range photogrammetry, the white uniform colouring of the surface and smooth texture required significant adjustments to the settings (e.g., aperture and exposure) to obtain a high-quality DEM, due to a lack of contrast between pixels, limiting the success of SDPS matching (Bertin et al., 2015). Therefore, we varied the amount of black dye in the other casts, partly to see the effect on the resultant DEMs and finally, to obtain a cast similar in colour to a natural river bed (Figure 3b–d). Once the resin had set (>12 hr), the mould can be peeled easily off the cast to leave the replica surface.

2.4 | DEM comparisons

To quantitatively assess the quality of the casting technique, DEMs were obtained of each cast when placed into the laboratory flume. Obtaining DEMs of both the natural surface and the replica surface for each studied topography allows for a DEM of difference (DoD) to be calculated by calculating the differences in elevations between each surface (e.g., the replica surface was subtracted from the natural surface). Surfaces were aligned during the calculations using corresponding particles in each DEM before the DoD was detrended linearly to remove any effect of experimental setup misalignment between DEM collections.

2.5 | Roughness statistics

Roughness statistics are frequently calculated to provide information regarding the surface aside from grain size and can be used as input parameters for hydraulic and morphodynamic models, along with flow resistance models (Aberle & Smart, 2003; Tuijnder & Ribberink, 2012). Here, bed-elevation distribution moments contained in probability distribution functions are calculated for both the natural and replica surface. These include skewness (indication to the degree of water working), kurtosis (measure of the degree of regularity of the bed),

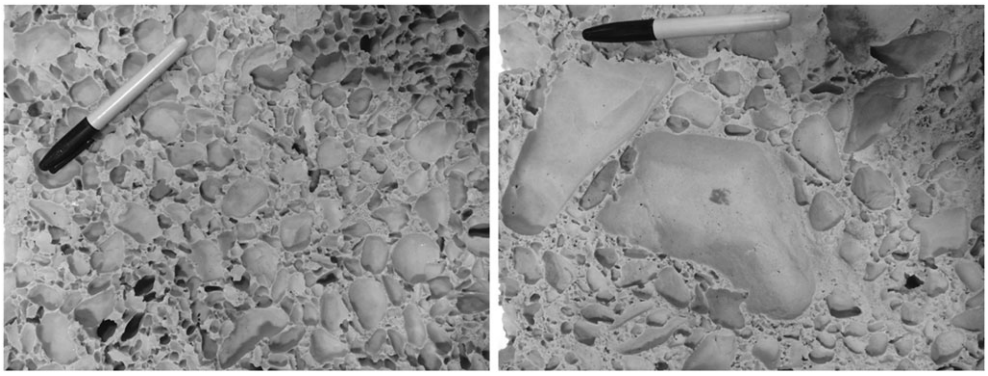

FIGURE 2 Negative imprint from the moulding process of Lab 1 (left) and Field 1 (right), which demonstrates a difference in the grain sizes replicated. For reference, the pen is 13.7 cm in length

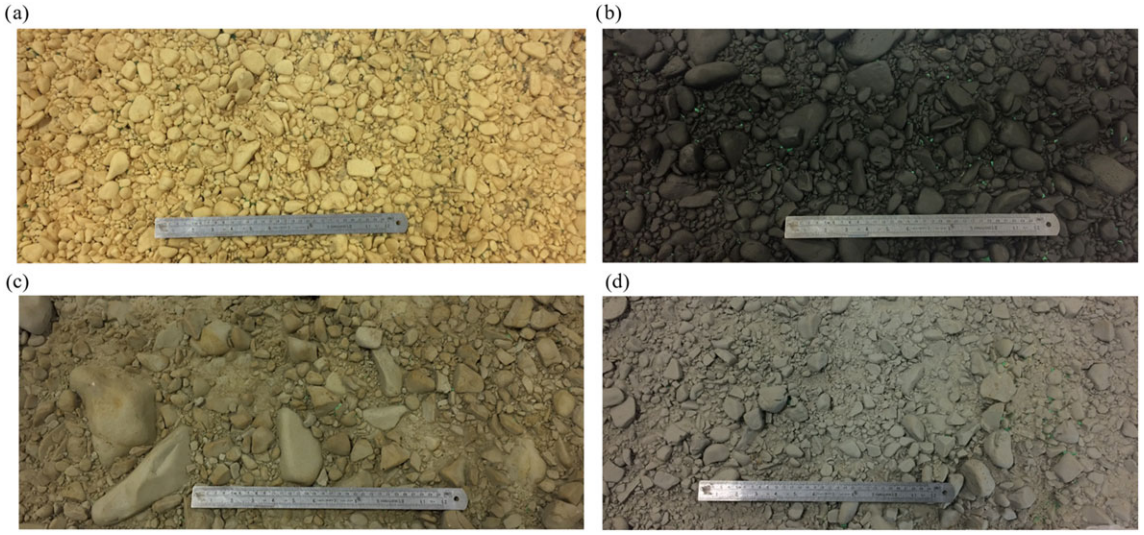

FIGURE 3 Photographs of all four casts presented throughout the paper: (a) Lab 1, (b) Lab 2, (c) Field 1, and (d) Field 2. The ruler is 30-cm long for reference [Colour figure can be viewed at wileyonlinelibrary.com]

standard deviation of elevations (vertical roughness length of the surface and indication of surface variability), and inclination index (I0). Inclination index is a characteristic of grain imbrication analysed from the signs of elevation changes between successive pairs of DEM points, where a positive value reflects particle imbrication (Millane, Weir, & Smart, 2006; Smart, Aberle, Duncan, & Walsh, 2004). These surface metrics are outlined and have been used in several studies to characterize the bed (Aberle & Nikora, 2006; Aberle & Smart, 2003; Coleman, Nikora, & Aberle, 2011; Noss & Lorke, 2016).

3 | RESULTS

3.1 | Assessing the quality of replica surfaces

Figure 4 shows DoDs for each surface, allowing an assessment to the accuracy of the surface replication. In all casts, there are strong similarities between the two surfaces. For all DoDs, the mean vertical absolute error lies approximately in the range of 3–4 mm, the maximum vertical error between 4 and 35 mm, and aggradation and erosion across the surface are between 37 and 43% (Table 1). Due to the similarities in values, it demonstrates there is no overall aggradation or erosion across any cast, and these values are attributed to particle dislodgement. All casts, except Field 2 (which has 46%), have >50% of values within a 3-mm difference that is larger than the 37% found in previous studies (Buffin-Bélanger et al., 2003). Overall, the statistics are consistent across the casts, suggesting consistency within the casting procedure. The dislodgement of individual particles at 350 mm (Lab 1), 300 mm (Lab 2), and 200 mm downstream (Field 2) is observed, likely from the moulding material knocking the particle during pouring, which we will explore in Section 4.1 below.

Roughness statistics for each surface (i.e., natural and replica) were compared with further assess the replicability of casting in the context of grain-roughness (Table 2). We observed changes in

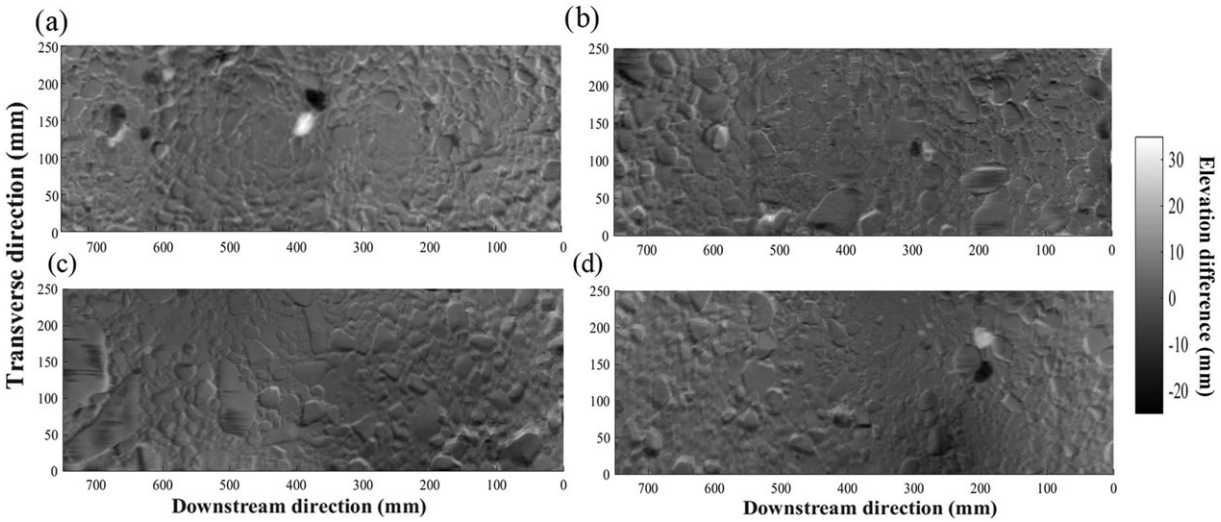

FIGURE 4 Digital elevation model of difference for each cast: (a) Lab 1, (b) Lab 2, (c) Field 1, and (d) Field 2. Colour bar represents the bed elevation difference in millimetres, where positive values represent aggradation on the replica surface

TABLE 1 Digital elevation model of difference data for each cast. Aggradation and erosion values demonstrate the percentage of the surface in which there were increased elevations on the cast (aggradation) or decrease in elevation on the cast (erosion)

DoD data	Lab 1	Lab 2	Field 1	Field 2
Mean vertical absolute error (mm)	3.05	2.93	3.15	4.09
Maximum vertical absolute error (mm)	25.37	34.91	4.33	24.36
Percentage of values within +/− 1 mm (%)	24.5	25.5	19.8	16.3
Percentage of values within +/− 3 mm (%)	60.9	63.0	55.8	46.3
Aggradation occurred across surface (%)	37	37	40	41
Erosion occurred across surface (%)	38	38	40	43

skewness across the replica surfaces, an increase in kurtosis (except Field 2) and a reduction in both standard deviation of elevations and range in elevations (except Lab 1). Inclination index switched direction (i.e., from negative to positive inclination index) for both Field casts, whereas Lab 1 remained negative and Lab 2 remained positive between surfaces. Mann–Whitney statistical testing demonstrated that these differences between the natural and replica surface are not statistically different ($p < 0.05$ confidence level). Using the roughness statistics, we therefore conclude that the casts are suitable replica of the roughness of the natural surfaces, both in the laboratory and the field.

3.2 | Morphological considerations for patch-scale studies

Figure 5 demonstrates how the construction of DEMs, obtained through close-range photogrammetry, is influenced by the presence of low-level scattered vegetation (Figure 5a). Figure 5b demonstrates with distortions in the DEM from 800 mm downstream, with higher elevations than the surrounding gravel followed by a region of high elevations resulting from noise in the DEM (~1,000 mm downstream). Distortions in the DEM could only be ascertained through visual inspection, as there is no ground truth available of the surface that can be used to assess DEM quality (Bertin et al., 2015). The DEM was cropped just prior to the vegetated area, making the DEM 750 mm in the downstream direction, instead of >1,000 mm.

Figure 5c demonstrates the differences in the distribution of bed elevations for the cropped DEM and the DEM containing the vegetation. The presence of vegetation results in a longer tail of the histogram (with bed elevations up to 60 mm) and an increased fraction of the surface containing negative bed elevations (Figure 5 c). Subsequently, roughness statistics were calculated for the raw DEM (with vegetation) and the cropped version. Higher skewness (1.0 compared with 0.7 without vegetation), kurtosis (22.7 compared with 4.1 without vegetation), standard deviation of elevation (10.7 mm compared with 8.9 mm without vegetation), and range in elevations (100.4 mm compared with 59.9 mm without vegetation) were observed in the DEM with vegetation present. The effect of vegetation is not assessed on inclination index; however, it is expected to have an effect. These roughness statistics were statistically similar (using Mann–Whitney tests), meaning that the cropped patch still adequately measured the grain roughness of the surface, yet without the areas of vegetation, there is a loss of detail in sediment patterns. However, as the focus of this study was on grain-scale roughness, the removal of vegetation was deemed appropriate.

4 | DISCUSSION

4.1 | Evaluating the replication of gravel-bed surfaces

We present the DoD between replica and natural surfaces, which previously have not been presented in those studies that have utilized the casting technique (Rice et al., 2014; Spiller et al., 2012), except in the initial outlines of the casting process (Buffin-Bélanger et al., 2003; Chandler et al., 2003). No DoDs for casts made of silicone rubber have been presented previously.

Subsequent use of the casting technique in experiments are summarized in Table 3, with advances to the technique enabling smaller grain sizes to be replicated. Work into evaluating the accuracy of the casting technique involved replicating golf balls and sandpaper, using laser scanning to obtain DEMs, and presenting the differences between the surfaces as histograms, before assessing hydraulic parameters between surfaces (Navaratnam, Aberle, & Spiller, 2016). Recent developments found good agreement between a gravel bed and cast, with the majority of the surface distributed within a range of 10 mm of surface elevation differences, with a total range of 40 mm in the difference between the two surfaces (Navaratnam, Aberle, Qin, & Henry, 2018).

TABLE 2 Roughness statistics for all natural surfaces, both in the laboratory and field, compared with their replica casts

	Lab 1		Lab 2		Field 1		Field 2	
Roughness statistic	Surface	Cast	Surface	Cast	Surface	Cast	Surface	Cast
Sk	0.34	0.29	0.47	0.58	0.34	0.75	0.95	0.90
Ku	3.17	3.19	3.22	3.44	3.48	3.74	5.34	5.21
σ_z (mm)	3.42	3.44	5.29	5.10	6.18	5.43	3.81	3.77
Range (mm)	36.96	33.34	45.25	45.99	61.29	61.73	43.76	51.09
I0	−0.012	−0.002	0.015	0.005	−0.001	0.056	−0.015	0.016

Note. These include skewness (Sk), kurtosis (Ku), the standard deviation of elevations (σ_z), the range in bed elevations, and inclination index (I0).

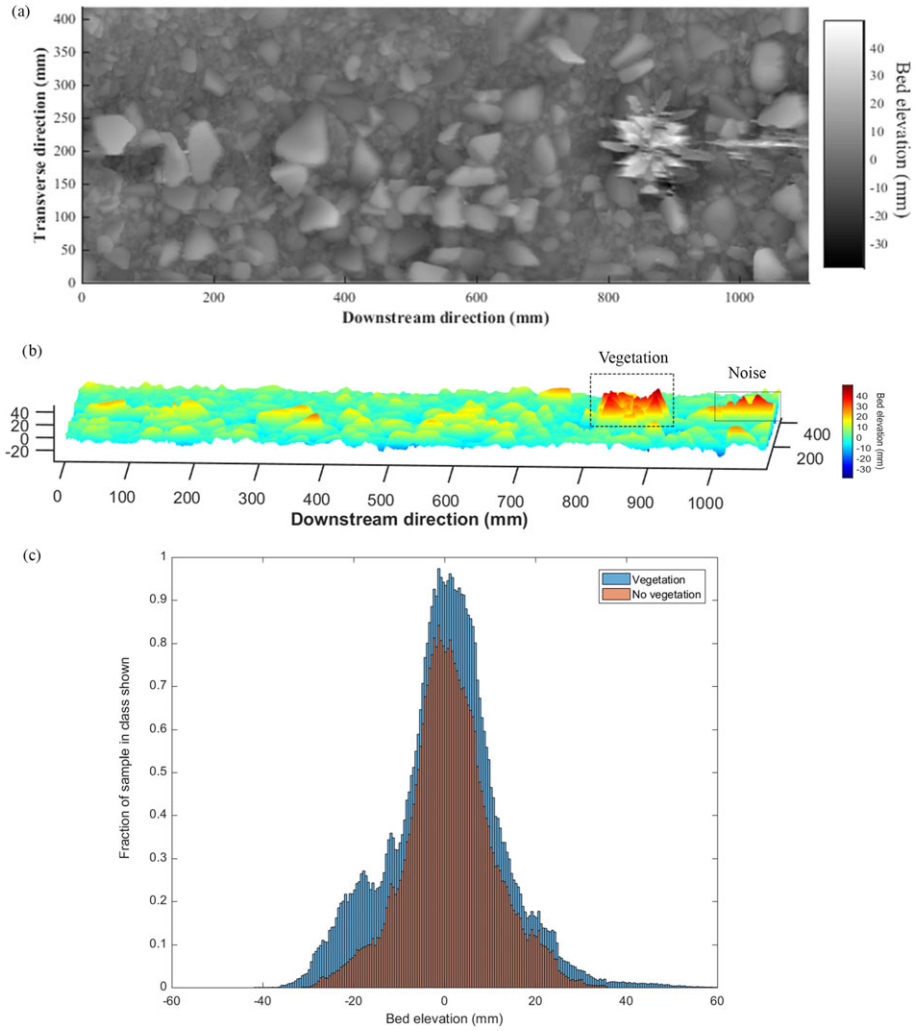

FIGURE 5 Presence of vegetation in digital elevation model (DEM) for example field surface visually resulting in errors in the DEM (a), due to vegetation elevation height and noise (b). Histogram of bed elevations for the DEM containing vegetation and the cropped DEM for roughness analysis (c) [Colour figure can be viewed at wileyonlinelibrary.com]

As demonstrated in our work, this casting technique can provide adequate replication of the surface topography (and ergo grain-scale roughness) of natural gravel-bed surfaces. DoDs display strong similarities in the surface, aside from several dislodged particles (Figure 4a, b, and d).

We postulate the reasoning for the displacement of these particles is a result of the silicone moulding material being poured onto the surface and the impact of the material causing dislodgement. This could especially be the case for the impact point of pouring (i.e., the location where the first of the liquid mould touched the surface). Attempts were made to pour the mould slowly and not focused on one location above the surface; however, due to the volume of the mould (>10 kg), there was a need to pour a significant volume within a time of 6–8 min (Spiller et al., 2012). This is due to the viscosity of the material increasing rapidly (i.e., within minutes), and it is imperative that the mould is viscous enough to reduce the movement of material but able to form the intricate details of the topography. Working on the same principles of sediment entrainment resulting from flow, the degree of packing across the surface will influence the mobility of stones, with surfaces that are tightly packed being more resistant to sediment entrainment (Ockelford & Haynes, 2013). Therefore, the ease at which particles can be displaced is likely related to the structure of packing, so it could be inferred that Lab 2 and Field 1 (Figure 4b and c) were more compact surfaces (i.e., greater packing density), meaning that particles did not become easily dislodged during the pouring of the mould. The lack of particle dislodgement presented in previous DoD is likely due to the larger grain sizes (D_{50} 50–65 mm compared with D_{50} 16–18 mm in this study) used (Buffin-Bélanger et al., 2003), indicating the larger grain sizes may not be as vulnerable to being dislodged from the moulding material.

Applications of the casting technique include multiple physical experiments undertaken to form a network of results (Table 3), and using fixed beds is advantageous for investigating flow structures and hydrodynamic forces (Cooper et al., 2017; Rice et al., 2014; Spiller et al., 2012). Although we currently recommend using the casting process for surface replication, there are opportunities in future research for the use of 3D printing (Viles, 2016) that could avoid the aforementioned issues encountered with the casting process (e.g., particle dislodgement). Presently, low volume models are suitable for 3D printing, however larger volume (such as the scale obtained using casting) requires expensive (>$100,000) 3D printers (Ishutov et al., 2018) and requires a certain level of expertise (Hasiuk, Harding, Renner, & Winer,

TABLE 3 Summary of studies that have used the casting procedure for experimental purposes

Paper	Year	Origin	Grain size (D_{50}) mm	Casting materials used	Size of cast (m)	Technique	Accuracies
Buffin-Bélanger et al.	2003	Field	50–65	Polyvinyl chloride (Gelflex™) and Polyurethane resin	1.0 × 2.0	Digital imagery	45 mm (<1 × D_{50})
Chandler et al.	2003	Field	50–65	Polyvinyl chloride (Gelflex™) and Polyurethane resin	1.0 × 2.0	Digital imagery	3–5 mm across surface 30 mm in places (<1 × D_{50})
Buffin-Bélanger et al.	2006	Field	17	Polyvinyl chloride (Gelflex™) and Polyurethane resin	2.0 × 1.0	Close-range photogrammetry	n/a
Spiller et al.	2012	Lab	3–5	Silicone rubber and two-component polyurethane pouring resin	1.6 × 2.0	n/a	n/a
Rice et al.	2014	Field	33	Polyvinyl chloride (Gelflex™) and Polyurethane resin	2.0 × 1.0	Close-range photogrammetry	n/a
Cooper et al.	2018	Lab	12.5–16.1	Polyvinyl chloride (Gelflex™) and polyurethane foam resin	0.40 × 0.40	Hand-held laser scanning	n/a
Navaratnam et al.	2018	Lab	3.5	Silicone rubber and two-component polyurethane pouring resin	1–2.3 × 1	Laser displacement metre	40 mm (~11 × D_{50})
Groom and Friedrich (this study)	2018	Lab and Field	16–18	Silicone rubber and two-component polyurethane pouring resin	0.90 × 0.35	Close-range photogrammetry	< 35 mm (~2 × D_{50})

2017). The feasibility of using laboratory experiments, field experiments, and numerical modelling in conjunction can provide a deeper understanding of the processes occurring at different scales (Yager et al., 2015), in order to progress scientific understanding and for river management applications.

4.2 | Morphological considerations for patch-scale studies

Close-range photogrammetry can be applied readily in the field, to obtain patch-scale topographic data with submillimetre resolution, for surface roughness studies (Bertin & Friedrich, 2016; Groom et al., 2018). For patch-scale morphological studies, it is vital to consider surrounding morphology for contextualisation. Man-made features are also important, including rock revetments, which are used to reduce bank erosion and flood risk (Angradi, Schweiger, Bolgrien, Ismert, & Selle, 2004) or artificial riffles that are incorporated during rehabilitation work for ecological purposes (Sear & Newson, 2004). An example of these features present in the Whakatiwai Stream is demonstrated in Figure 6.

Patch-scale research using close-range photogrammetry supplemented with larger-scale data obtained by SfM could provide this contextualisation. This technique has been applied in the field covering the fluvial mesoscale (e.g., >10 m–km) (Javernick, Brasington, & Caruso, 2014; Woodget & Austrums, 2017; Woodget, Carbonneau, Visser, & Maddock, 2015; Woodget, Fyffe, & Carbonneau, 2018), with DEM resolutions ranging from 10–50 mm (James, Robson, D'oleire-Oltmanns, & Niethammer, 2017; Javernick et al., 2014). However, a wide range inaccuracies (from subdecimetre to over 1 m) have been reported in geomorphic studies using SfM (Cook, 2017). Whilst SfM has the capabilities to produce data quality comparable to that of terrestrial laser scanning, as found in flume studies (Morgan, Brogan, & Nelson, 2017), in order to achieve subcentimetre precisions, field surveys require decreased flying heights that limit the spatial coverage (James et al., 2017). Previous SfM studies to quantify grain size over the reach scale have collected data identifying geomorphic changes of 19 mm, which was less than the median grain size (D_{50} = 31 mm) at a DEM resolution of 0.25 m (Vázquez-Tarrío, Borgniet, Liébault, & Recking, 2017). More recently, precision lower than 1 mm has been obtained on grain sizes ranging from 10 to 180 mm (Woodget & Austrums, 2017) providing evidence of the developments to the SfM technique. Based on these advances, using close-range photogrammetry to obtain detailed submillimetre grain-scale roughness information and SfM to quantify the larger scale is an exciting prospect for emerging research, with a focus on developing geomorphic insights and advancing geomorphic science (Entwistle, Heritage, & Milan, 2018).

The effect of artificial features can be investigated using SfM. Coarser DEM resolutions (e.g., 50 mm) are suited for geomorphic change techniques to assess the effect of river restoration practices (Marteau, Vericat, Gibbins, Batalla, & Green, 2017). However, there are issues with vegetation in geomorphic change studies due to seasonal changes, and the effect of vegetation in SfM data is dependent on the type and density of vegetation (Cook, 2017). The inclusion of vegetation in terrestrial laser scanning data can result in artefacts that can be removed through visual inspection; however, it was noted that there was considerable noise associated with backscatter from vegetation, which is likely to result in the overestimation of volume changes from DoDs over large scales (Brasington et al., 2012).

In patch-scale gravel-bed research (e.g., using close-range photogrammetry), densely vegetated areas of the surface are avoided; however, smaller scattered areas of low-level vegetation could be present in patches. This results in several difficulties during analysis, including influencing DEM quality due to the presence of noise (Figure 5a and b) that are not encountered in non-vegetated laboratory experiments (Bertin & Friedrich, 2014). The removal of vegetation from the DEM resulted in the removal of higher bed elevations (e.g., less extreme elevations in the surface distribution) and less of the surface containing negative bed elevations (Figure 5c). However, the cropped DEM provided statistically similar roughness statistics compared with the DEM with vegetation, suggesting that across this surface even though the patch size was smaller, it adequately captured the grain roughness

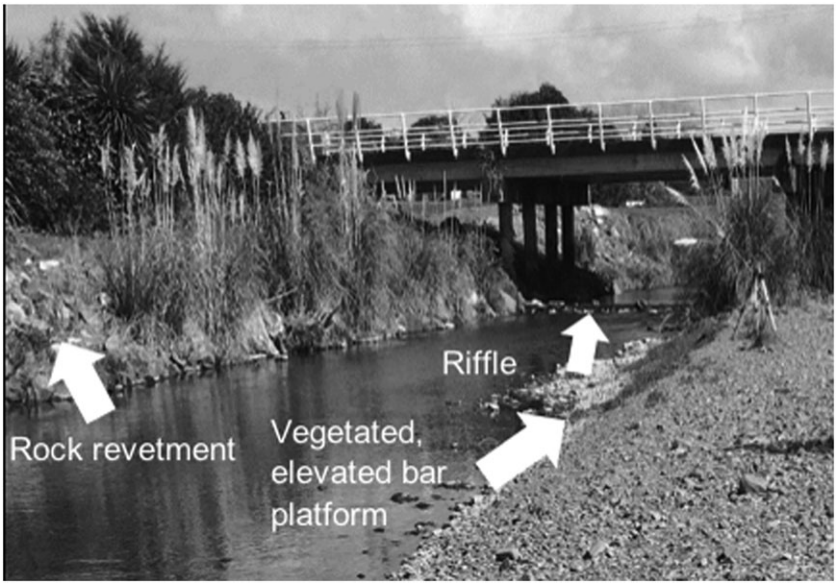

FIGURE 6 Annotated photograph of key morphological features from an example of the Whakatiwai Stream, New Zealand

of the patch. The extent (and type) of vegetation across a patch will vary, and in some cases, removal of vegetation in this manner may be inappropriate and provide differences in the roughness quantified across a patch.

Vegetation is a key influence in sedimentation patterns (Blacknell, 1982) and significantly contributes to the surface roughness, along with an influence on flow properties (Hardy, 2006; Smith, 2014). Therefore, the question of whether vegetation should be incorporated into fluvial roughness research needs addressing. The potential for whether the casting procedure can adequately replicate the vegetation occurring in natural gravel patches or how vegetation influences the replica surface is an avenue for future exploration.

5 | CONCLUSION

DEMs of difference (DoDs), captured using high-resolution close-range photogrammetry, are presented to quantitatively assess the replicability of gravel-bed surfaces using the casting process (with mean vertical errors of 3–4 mm). We advocate the use of the casting technique to replicate the surface of both laboratory and field environments, despite the observation of particle dislodgment (due to pouring the mould). This enables natural surfaces to be analysed in a controlled laboratory environment, providing a bridge between the existing lab-field interface in fluvial morphology.

Contextualisation of patch-scale field research is required, as morphological factors including vegetation influence process interpretation and data quality (demonstrated by the presence of noise in DEMs), however are omitted from laboratory studies or are difficult to replicate. The ability to replicate surfaces and implementing the same technique for data analysis (e.g., close-range photogrammetry), facilitates comparison studies between environments to bridge the lab-field interface in fluvial morphology.

ACKNOWLEDGEMENTS

The authors thank Stéphane Bertin and Wei Li for their assistance in the collection of field data. The study was partly funded by the Marsden Fund (Grant No. UOA1412), administered by the Royal Society of New Zealand.

ORCID

Jane Groom http://orcid.org/0000-0001-6938-483X
Heide Friedrich http://orcid.org/0000-0002-6419-5973

REFERENCES

Aberle, J., & Nikora, V. (2006). Statistical properties of armored gravel bed surfaces. *Water Resources Research*, *42*, W11414.

Aberle, J., Nikora, V., Henning, M., Ettmer, B., & Hentschel, B. (2010). Statistical characterization of bed roughness due to bed forms: A field study in the Elbe River at Aken, Germany. *Water Resources Research*, *46*, W03521.

Aberle, J., & Smart, G. M. (2003). The influence of roughness structure on flow resistance on steep slopes. *Journal of Hydraulic Research*, *41*, 259–269. https://doi.org/10.1080/00221680309499971

Angradi, T. R., Schweiger, E. W., Bolgrien, D. W., Ismert, P., & Selle, T. (2004). Bank stabilization, riparian land use and the distribution of large woody debris in a regulated reach of the upper Missouri River, North Dakota, USA. *River Research and Applications*, *20*, 829–846. https://doi.org/10.1002/rra.797

Ashworth, P. J., & Ferguson, R. I. (1986). Interrelationships of channel processes, changes and sediments in a proglacial braided river. *Geografiska Annaler. Series A, Physical Geography*, *68*, 361–371. https://doi.org/10.1080/04353676.1986.11880186

Basile, A., Ciollaro, G., & Coppola, A. (2003). Hysteresis in soil water characteristics as a key to interpreting comparisons of laboratory and field measured hydraulic properties. *Water Resources Research*, *39*. https://doi.org/10.1029/2003WR002432

Bertin, S. (2016). Developments in photogrammetric remote sensing for grain-scale fluvial morphology studies. *ResearchSpace@ Auckland.*.

Bertin, S., & Friedrich, H. (2014). Measurement of gravel-bed topography: Evaluation study applying statistical roughness analysis. *Journal of Hydraulic Engineering*, *140*, 269–279. https://doi.org/10.1061/(ASCE)HY.1943-7900.0000823

Bertin, S., & Friedrich, H. (2016). Field application of close-range digital photogrammetry (CRDP) for grain-scale fluvial morphology studies. *Earth Surface Processes and Landforms*, *41*, 1358–1369. https://doi.org/10.1002/esp.3906

Bertin, S., Friedrich, H., & Delmas, P. (2016). A merging solution for close-range DEMs to optimize surface coverage and measurement

resolution. *Photogrammetric Engineering & Remote Sensing*, *82*, 31–40. https://doi.org/10.14358/PERS.83.1.31

Bertin, S., Friedrich, H., Delmas, P., & Chan, E. (2013). The use of close-range digital stereo-photogrammetry to measure gravel-bed topography in a laboratory environment. Proceedings of the 35th IAHR congress, Chengdu, China, 2013.

Bertin, S., Friedrich, H., Delmas, P., Chan, E., & Gimel'farb, G. (2015). Digital stereo photogrammetry for grain-scale monitoring of fluvial surfaces: Error evaluation and workflow optimisation. *ISPRS Journal of Photogrammetry and Remote Sensing*, *101*, 193–208. https://doi.org/10.1016/j.isprsjprs.2014.12.019

Blacknell, C. (1982). Morphology and surface sedimentary features of point bars in Welsh gravel-bed rivers. *Geological Magazine*, *119*, 181–192. https://doi.org/10.1017/S0016756800025863

Brasington, J., & Smart, R. M. A. (2003). Close range digital photogrammetric analysis of experimental drainage basin evolution. *Earth Surface Processes and Landforms*, *28*, 231–247. https://doi.org/10.1002/esp.480

Brasington, J., Vericat, D., & Rychkov, I. (2012). Modeling river bed morphology, roughness, and surface sedimentology using high resolution terrestrial laser scanning. *Water Resources Research*, *48*, 1–18.

Buffin-Bélanger, T., Reid, I., Rice, S., Chandler, J. H., & Lancaster, J. (2003). A casting procedure for reproducing coarse-grained sedimentary surfaces. *Earth Surface Processes and Landforms*, *28*, 787–796. https://doi.org/10.1002/esp.490

Butler, J. B., Lane, S. N., & Chandler, J. H. (1998). Assessment of DEM quality for characterizing surface roughness using close range digital photogrammetry. *The Photogrammetric Record*, *16*, 271–291. https://doi.org/10.1111/0031-868X.00126

Butler, J. B., Lane, S. N., & Chandler, J. H. (2001). Characterization of the structure of river-bed gravels using two-dimensional fractal analysis. *Mathematical Geology*, *33*, 301–330. https://doi.org/10.1023/A:1007686206695

Carbonneau, P. E., Lane, S. N., & Bergeron, N. E. (2003). Cost-effective non-metric close-range digital photogrammetry and its application to a study of coarse gravel river beds. *International Journal of Remote Sensing*, *24*, 2837–2854. https://doi.org/10.1080/01431160110108364

Chandler, J. H., Buffin-Bélanger, T., Rice, S., Reid, I., & Graham, D. J. (2003). The accuracy of a river bed moulding/casting system and the effectiveness of a low-cost digital camera for recording river bed fabric. *The Photogrammetric Record*, *18*, 209–223. https://doi.org/10.1111/0031-868X.t01-1-00008

Chandler, J. H., Shiono, K., Rameshwaren, P., & Lane, S. N. (2001). Measuring flume surfaces for hydraulics research using a Kodak DCS460. *The Photogrammetric Record*, *17*, 39–61. https://doi.org/10.1111/0031-868X.00167

Church, M., Hassan, M. A., & Wolcott, J. F. (1998). Stabilizing self-organized structures in gravel-bed stream channels: Field and experimental observations. *Water Resources Research*, *34*, 3169–3179. https://doi.org/10.1029/98WR00484

Coleman, S. E., Nikora, V. I., & Aberle, J. (2011). Interpretation of alluvial beds through bed-elevation distribution moments. *Water Resources Research*, *47*, W11505.

Cook, K. L. (2017). An evaluation of the effectiveness of low-cost UAVs and structure from motion for geomorphic change detection. *Geomorphology*, *278*, 195–208. https://doi.org/10.1016/j.geomorph.2016.11.009

Cooper, J. R., Ockleford, A., Rice, S. P., & Powell, D. M. (2017). Does the permeability of gravel river beds affect near-bed hydrodynamics? *Earth Surface Processes and Landforms*, *43*, 943–955.

Detert, M., & Weitbrecht, V. (2012). Automatic object detection to analyze the geometry of gravel grains–a free stand-alone tool. *Proceedings of River Flow*, *2012*, 595–600.

Entwistle, N., Heritage, G., & Milan, D. (2018). Recent remote sensing applications for hydro and morphodynamic monitoring and modelling. *Earth Surface Processes and Landforms*, *43*, 2283–2291. https://doi.org/10.1002/esp.4378

Gimel'farb, G. (2002). Probabilistic regularisation and symmetry in binocular dynamic programming stereo. *Pattern Recognition Letters*, *23*, 431–442. https://doi.org/10.1016/S0167-8655(01)00175-1

Groom, J., Bertin, S., & Friedrich, H. (2018). Assessing intra-bar variations in grain roughness using close-range photogrammetry. *Journal of Sedimentary Research*, *88*, 555–567. https://doi.org/10.2110/jsr.2018.30

Hardy, R. J. (2006). Fluvial geomorphology. *Progress in Physical Geography*, *30*, 553–567. https://doi.org/10.1191/0309133306pp498pr

Hasiuk, F. J., Harding, C., Renner, A. R., & Winer, E. (2017). TouchTerrain: A simple web-tool for creating 3D-printable topographic models. *Computers & Geosciences*, *109*, 25–31. https://doi.org/10.1016/j.cageo.2017.07.005

Hodge, R., Brasington, J., & Richards, K. (2009a). Analysing laser-scanned digital terrain models of gravel bed surfaces: Linking morphology to sediment transport processes and hydraulics. *Sedimentology*, *56*, 2024–2043. https://doi.org/10.1111/j.1365-3091.2009.01068.x

Hodge, R., Brasington, J., & Richards, K. (2009b). In situ characterization of grain-scale fluvial morphology using Terrestrial Laser Scanning. *Earth Surface Processes and Landforms*, *34*, 954–968.

Huang, G.-H., & Wang, C.-K. (2012). Multiscale geostatistical estimation of gravel-bed roughness from terrestrial and airborne laser scanning. *Geoscience and Remote Sensing Letters, IEEE*, *9*, 1084–1088. https://doi.org/10.1109/LGRS.2012.2189351

Ishutov, S., Jobe, T. D., Zhang, S., Gonzalez, M., Agar, S. M., Hasiuk, F. J., … Chalaturnyk, R. (2018). Three-dimensional printing for geoscience: Fundamental research, education, and applications for the petroleum industry. *AAPG Bulletin*, *102*, 1–26. https://doi.org/10.1306/0329171621117056

James, M. R., Robson, S., D'oleire-Oltmanns, S., & Niethammer, U. (2017). Optimising UAV topographic surveys processed with structure-from-motion: Ground control quality, quantity and bundle adjustment. *Geomorphology*, *280*, 51–66. https://doi.org/10.1016/j.geomorph.2016.11.021

Javernick, L., Brasington, J., & Caruso, B. (2014). Modeling the topography of shallow braided rivers using structure-from-motion photogrammetry. *Geomorphology*, *213*, 166–182. https://doi.org/10.1016/j.geomorph.2014.01.006

Klotz, D., Seiler, K. P., Moser, H., & Neumaier, F. (1980). Dispersivity and velocity relationship from laboratory and field experiments. *Journal of Hydrology*, *45*, 169–184. https://doi.org/10.1016/0022-1694(80)90018-9

Lane, S. N., James, T. D., & Crowell, M. D. (2000). Application of digital photogrammetry to complex topography for geomorphological research. *The Photogrammetric Record*, *16*, 793–821. https://doi.org/10.1111/0031-868X.00152

Marteau, B., Vericat, D., Gibbins, C., Batalla, R. J., & Green, D. R. (2017). Application of structure-from-motion photogrammetry to river restoration. *Earth Surface Processes and Landforms*, *42*, 503–515. https://doi.org/10.1002/esp.4086

Millane, R. P., Weir, M. I., & Smart, G. M. (2006). Automated analysis of imbrication and flow direction in alluvial sediments using laser-scan data. *Journal of Sedimentary Research*, *76*, 1049–1055. https://doi.org/10.2110/jsr.2006.098

Morgan, J. A., Brogan, D. J., & Nelson, P. A. (2017). Application of Structure-from-Motion photogrammetry in laboratory flumes. *Geomorphology*, *276*, 125–143. https://doi.org/10.1016/j.geomorph.2016.10.021

Navaratnam, C. U., Aberle, J., Qin, J., & Henry, P.-Y. (2018). Influence of gravel-bed porosity and grain orientation on bulk flow resistance. *Water*, *10*, 561. https://doi.org/10.3390/w10050561

Navaratnam, C. U., Aberle, J., & Spiller, S. (2016). Geometric and hydraulic assessment of the accuracy of a bed moulding.

Noss, C., & Lorke, A. (2016). Roughness, resistance, and dispersion: Relationships in small streams. *Water Resources Research*, *52*, 2802–2821. https://doi.org/10.1002/2015WR017449

Ockelford, A. M., & Haynes, H. (2013). The impact of stress history on bed structure. *Earth Surface Processes and Landforms*, *38*, 717–727. https://doi.org/10.1002/esp.3348

Piégay, H., Kondolf, G. M., Minear, J. T., & Vaudor, L. (2015). Trends in publications in fluvial geomorphology over two decades: A truly new era in the discipline owing to recent technological revolution? *Geomorphology*, *248*, 489–500. https://doi.org/10.1016/j.geomorph.2015.07.039

Rice, S. P., Buffin-Bélanger, T., & Reid, I. (2014). Sensitivity of interfacial hydraulics to the microtopographic roughness of water-lain gravels. *Earth Surface Processes and Landforms*, *39*, 184–199. https://doi.org/10.1002/esp.3438

Rice, S. P., Lancaster, J., & Kemp, P. (2010). Experimentation at the interface of fluvial geomorphology, stream ecology and hydraulic engineering and the development of an effective, interdisciplinary river science. *Earth Surface Processes and Landforms*, *35*, 64–77. https://doi.org/10.1002/esp.1838

Sear, D. A., & Newson, M. D. (2004). The hydraulic impact and performance of a lowland rehabilitation scheme based on pool–riffle installation: The River Waveney, Scole, Suffolk, UK. *River Research and Applications*, *20*, 847–863. https://doi.org/10.1002/rra.791

Smart, G., Aberle, J., Duncan, M., & Walsh, J. (2004). Measurement and analysis of alluvial bed roughness. *Journal of Hydraulic Research*, *42*, 227–237.

Smith, M. W. (2014). Roughness in the Earth Sciences. *Earth-Science Reviews*, *136*, 202–225. https://doi.org/10.1016/j.earscirev.2014.05.016

Spiller, S., Rüther, N., & Baumann, B. (2012). Artificial reproduction of the surface structure in a gravel bed. *Proceedings of 2nd International Association for Hydraulic Research (IAHR) Europe Congress*, Munich, Germany, 27–29.

Thompson, R. C., Norton, T. A., & Hawkins, S. J. (1998). The influence of epilithic microbial films on the settlement of Semibalanus balanoides cyprids—A comparison between laboratory and field experiments. *Hydrobiologia*, *375*, 203–216.

Tuijnder, A. P., & Ribberink, J. S. (2012). Experimental observation and modelling of roughness variation due to supply-limited sediment transport in uni-directional flow. *Journal of Hydraulic Research*, *50*, 506–520. https://doi.org/10.1080/00221686.2012.719201

Vázquez-Tarrío, D., Borgniet, L., Liébault, F., & Recking, A. (2017). Using UAS optical imagery and SfM photogrammetry to characterize the surface grain size of gravel bars in a braided river (Vénéon River, French Alps). *Geomorphology*, *285*, 94–105. https://doi.org/10.1016/j.geomorph.2017.01.039

Viles, H. (2016). Technology and geomorphology: Are improvements in data collection techniques transforming geomorphic science? *Geomorphology*, *270*, 121–133. https://doi.org/10.1016/j.geomorph.2016.07.011

Wickham, R., & Petrie, J. (2015). Quantifying the spatial variability of stream bed grain size distributions.

Woodget, A. S., & Austrums, R. (2017). Subaerial gravel size measurement using topographic data derived from a UAV-SfM approach. *Earth Surface Processes and Landforms*, *42*, 1434–1443. https://doi.org/10.1002/esp.4139

Woodget, A. S., Carbonneau, P. E., Visser, F., & Maddock, I. P. (2015). Quantifying submerged fluvial topography using hyperspatial resolution UAS imagery and structure from motion photogrammetry. *Earth Surface Processes and Landforms*, *40*, 47–64. https://doi.org/10.1002/esp.3613

Woodget, A. S., Fyffe, C., & Carbonneau, P. E. (2018). From manned to unmanned aircraft: Adapting airborne particle size mapping methodologies to the characteristics of sUAS and SfM. *Earth Surface Processes and Landforms*, *43*, 857–870. https://doi.org/10.1002/esp.4285

Yager, E. M., Kenworthy, M., & Monsalve, A. (2015). Taking the river inside: Fundamental advances from laboratory experiments in measuring and understanding bedload transport processes. *Geomorphology*, *244*, 21–32. https://doi.org/10.1016/j.geomorph.2015.04.002

Yochum, S. E., Bledsoe, B. P., Wohl, E., & David, G. C. L. (2014). Spatial characterization of roughness elements in high-gradient channels of the Fraser Experimental Forest, Colorado, USA. *Water Resources Research*, *50*, 6015–6029. https://doi.org/10.1002/2014WR015587

Zhang, Z. (2000). A flexible new technique for camera calibration. *IEEE Transactions on Pattern Analysis and Machine Intelligence*, *22*, 1330–1334. https://doi.org/10.1109/34.888718

How to cite this article: Groom J, Friedrich H. Bridging the lab-field interface in fluvial morphology at patch-scale: Using close-range photogrammetry to assess surface replication and vegetation influence. *River Res Applic*. 2018;34:1328–1337. https://doi.org/10.1002/rra.3370